

Nonlinear Instability Modelling of a Nonlocal Strain Gradient Functionally Graded Capacitive Nano-Bridge Under Intermolecular Forces in Thermal Environment

Ilgar Jafarsadeghi-pournaki^a, Ghader Rezazadeh^{b*}, Rasool Shabani^c

^{a,b,c} Mechanical Engineering Department, Urmia University, Iran

^{b*} g.rezazadeh@urmia.ac.ir

Abstract This paper developed a theoretical model directed towards investigation of the static pull-in instability of functionally graded (FG) electrostatic nano-bridge under the influence of electrostatic and intermolecular forces in thermal environment via nonlocal strain gradient theory (NLSGT) of elasticity and Euler-Bernoulli beam theory in conjunction with the nonlinear geometric effect resulting from mid-plane stretching. Material properties of FG nano-beam is assumed to vary gradually along the thickness direction according to simple power-law form. With the purpose of eliminating the coupling between the stretching and bending due to the asymmetrical material variation along the thickness, a new surface reference is introduced. The nonlinear integro-differential governing equation is derived utilizing minimum total potential energy principle, linearized by means of the step-by-step linearization method (SSLM) and solved by Galerkin based weighted residual method. The numerical investigations are performed while the emphasis is placed on studying the effect of various parameters including: nonlocal parameter, material characteristic length scale, material gradient index, thermal effect, intermolecular forces on the static pull-in instability of FG nano-beam. To establish the validity of the present formulation, a comparison is conducted with experimental and numerical results reported in previous studies.

Keywords: Pull-in, instability, functionally graded, NEMS, nonlocal strain gradient theory

1 Introduction

Application of DC voltage in Nano-Electro-Mechanical systems (NEMS) has an upper limit such that the elastic restoring force in the deformable beam and electrostatic force cannot be balanced by each other, thereupon, the stable equilibrium positions of the micro beam vanishes. This famous phenomenon called pull-in instability observed experimentally and the critical voltage corresponding to this instability is called the pull-in voltage (Zamanzadeh et al. 2013; Jafarsadeghi et al. 2014).

The small-size scales corresponding micro- and nano- technologies are often adequately small to cause doubt on the implementation of classical continuum mechanics for nanostructures. Because they does not determine contributions of length scale effects which are important in investigating of nano-beams. Explanation of size-dependency is still an interesting issue in modeling of micro- and nano- structures. In general, there are two kinds of theories to figure out the mechanical behavior of these structures including: the nonlocal stress gradient theory and the strain gradient theory. These theories describe two completely different physical characteristics of materials and structures at micro- and nano-scale (Lu et al. 2016), the first one is a softening model and the second one is hardening. The nonlocal elasticity theory was proposed by Eringen (1983) to explain scale effect in elasticity by assuming the stress field in each point of a solid body to be a function of strains of all adjacent points besides strain state in that desired point. In this way, the internal size scale could be considered in the constitutive equations simply as a material parameter. This theory characterizes only softening effect. However, the effect of the stiffness enhancement, which is reported from the experimental and the theoretical studies cannot be taken into consideration by the nonlocal elasticity theory (Şimşek 2016). The modified strain gradient theory (MSGT) developed by Lam et al. (2015), assume that the materials must be considered as atoms with higher-order deformation mechanism at micro/nano scale rather than just modelled them as collections of points. The gradient elasticity theories add some additional higher-order strain gradient terms to the classical equations of elasticity to evaluate the behavior of higher-order strain gradients (Li et al. 2016). By considering what was discussed so far, it can be concluded that in order to establish the real size-dependent mechanical behavior, it is crucial to combine the nonlocal elasticity theory and the strain gradient. To generalize the Eringen's nonlocal elasticity model, the nonlocal strain gradient elasticity theory (NSGT) is introduced by considering a higher-order strain tensor with nonlocality into the stored energy function. The proposed theory is privileged because the classical nonlocal elasticity is impotent to capture nonlocality of higher-order stresses and common strain gradient theory to include higher-order strain gradients (Lim et al. 2015). In comparison with nonlocal elasticity, a new parameter in NSGT is appeared as representative of the effects of strain gradient field which has never been put forward in Eringen's theory. This novelty compensates the lack of stiffness-hardening influence in nonlocal elasticity.

Numerous models were developed to study the behavior of FG or homogenous micro- and nano- structures based on nonlocal continuum theory or strain gradient elasticity theory. The study of the small scale effect on the pull-in instability of nano-switches subjected to electrostatic and intermolecular forces was dealt with in the paper of Mousavi et al. (2012) using generalized differential quadrature method. The pull-in instability of nano-switches under intermolecular and electrostatic forces via hybrid nonlocal Euler-Bernoulli beam model was carried out by Taghavi and Nahvi (2013). Their results revealed that the Eringen's nonlocal beam model produces unreasonable pull-in voltages, minimum gaps and detachment lengths, that's why they use hybrid nonlocal beam model to resolve these shortcomings. Jafarsadeghi-pournaki et al. (2014) studied the static pull-in instability of FG capacitive nano-beam subjected to an electrostatic force and thermal moment via the nonlocal elasticity theory. They concluded that for a cantilever beam, the small scale parameter regarding nonlocal stress gradients increases the value of pull-in voltage, that's mean, the small scale effect contribute to the pull-in instability of cantilever and clamped-clamped beams in quite different ways. Utilizing nonlocal and strain gradient elasticity theories separately, the static behavior of electrically actuated micro and nano-beams were conducted by Maani Miandoab et al. (2015). In their study, the experimental voltages for static pull-in of different micro- and nano-beams are used to estimate the silicon Young's modulus, nonlocal and length scale parameters. Karimipour et al. (2015) employing Casimir force considered couple stress theory to modelling the nano-bridge and nano-cantilever actuators with double-sided actuating electrodes. Tadi Beni et al. (2015) presented a mathematical modeling to study the size dependent instability of nanostructures considering the effect of van der Waals intermolecular force on the basis of modified strain gradient theory. In other work, under the influence of electrostatic and intermolecular forces, static pull-in instability of a FG nano-cantilever using the strain gradient theory was studied by Ataei and Tadi Beni (2016). They demonstrate that the modified strain gradient theory predicts a higher pull-in voltage compared with the modified couple stress theory and the classical theory. Soltanrezaee et al. (2016) scrutinized the influences of length scale related to modified couple stress theory, surface elasticity, fringing field, residual surface stress, the geometrically nonlinear deformation as well as the location/length of the actuated electrode. With the aim of tuning the pull-in instability, a double-sided cantilever nano-wire (suspended between two stationary substrate plates), including the Casimir and partial electrostatic attractions were developed by Soltanrezaee and Afrashi (2016) on the basis of couple stress theory. Pull-in instability of double clamped micro-beams under dispersion forces in the presence of thermal and residual stress effects using nonlocal elasticity theory was presented by Tavakolian et al. (2017).

To assess the true effect of the two length scales on the mechanical and physical responses of size-dependent structures, there is few published studies in size dependent models presented in NSGT. Li and Hu (2015) developed a size-dependent nonlinear Euler–Bernoulli beam formulation via the nonlocal strain gradient theory to derive the post-buckling deflections and critical buckling forces of simply supported size-dependent beams. The comprehensive size-dependent vibration analysis of nano-beams based on the NSGT can be accessed by studying the recent works of by Li et al. (2016), Şimşek (2016) and Lu et al. (2017). Buckling analysis of size-dependent shear-deformable curved FG nano-beams via NSGT is conducted by Ebrahimi and barati (2017). Wave propagation responses of smart FG magneto-electro-elastic nano-plates via NSGT is performed by Ebrahimi and dabbagh (2017). More recently, Yang et al. (2017) investigated the dynamic pull-in instability of functionally graded carbon nanotubes (FGCNTs) reinforced nano-actuator by jointly using the nonlocal stress gradient and strain gradient theories. They employed a higher order corrected model of electrostatic force with fringing field effect accounting for large gap and geometrical nonlinearity. They also studied effect of nonlocality and strain gradient elasticity at the same time on dynamic pull-in behavior of FG nano-tubes reinforced nano-actuator considering damping effect. Their study confirmed that the frequencies decline with the increase of nonlocal parameter while increases with the increase of size effect regarding strain gradient theory Yang et al. (2017).

By taking what was discussed so far about the background into consideration, it can be concluded that a great deal of attention has been focused on studying of the static pull-in behavior of FG or homogenous nano-structures considering classic and non-classic models. Moreover, to study the dynamic behavior of nano-structures the theory newly proposed by Lim et al. (2015) widely has been used. However, to the best of the author's knowledge, no work has been devoted studying the nonlinear static pull-in behavior of FG nano-bridges employing NSGT while the intermolecular forces and temperature changes are considered. Using a Galerkin based step by step linearization method, nonlinear static deflection equation was solved and results are obtained in order to investigate the effects of nonlocal parameter, strain gradient parameter, Casimir and Van der Walls forces and temperature variation on the static pull-in instability. In addition, the solution validity is checked by comparing the results with different methods and experimental results published in the previous works which a reasonable good agreement is observed. The present NSGT developed model may be used together with different analytical and numerical methods to study the static behavior of nanostructures made of FG materials.

2 Theory and formulation

2.1 Functionally graded materials

Figure 1 depicts a FG nano-bridge separated from a fixed ground plate as a substrate by an initial gap. The clamped-clamped nano-beam deflects toward the underlying fixed electrode owing to the electrostatic and intermolecular forces. It should be noted that due to the variation in volume fractions of material phases the neutral axis of a FG nano-beam may not coincide with its mid-axis which causes bending-extension coupling. However, if the position of the physical neutral surface is determined and the origin of the coordinate system is fixed to the physical neutral surface, the material properties become symmetric about the physical neutral surface and the bending-extension coupling will reach zero. In order to specify the position of the new reference surface, two different coordinates, z and \bar{z} , are defined from the middle surface and from the new reference surface, respectively, as shown in Fig. 1. It is worth pointing out that the new reference surface defined by z , is not the neutral surface of the nano-beam owing to the nonlinear nature of the problem.

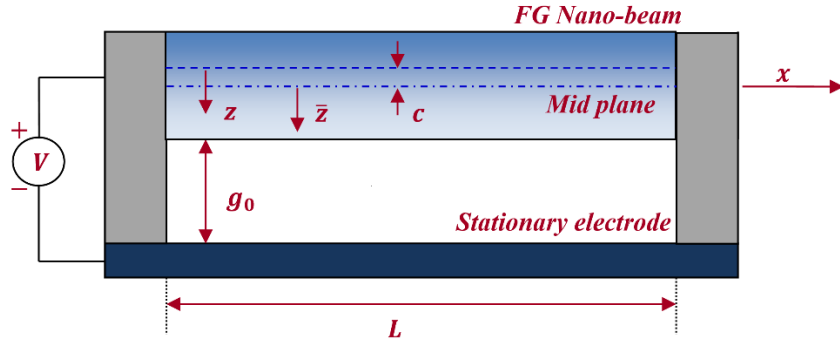


Fig. 1 Schematic representation of functionally graded capacitive nano-bridge.

Suppose that FG beam is made of two different materials in which the material property varies continuously according to the simple power-law form through the beam thickness. Based on the rule of mixture, the effective material properties P can be given by:

$$P = P_U V_U + P_L V_L \quad (1)$$

Where P_U and P_L are the corresponding material property at the upper and lower surfaces of the beam and V_U and V_L refer the volume fractions of the upper and lower, respectively, related by the classical ($V_U + V_L = 1$) relation. Considering the volume fraction on the basis of power-law form ($V_U = [(z_c + c) / h + 0.5]^k$), the distribution of a material property P across the thickness is given as follow:

$$P(\bar{z}) = (P_U - P_L) \left(\frac{\bar{z}}{h} + \frac{1}{2} \right)^k + P_L \quad (2)$$

In which k is a non-negative parameter prescribing the material variation profile through the thickness of the nano-beam. The new reference surface can be specified as:

$$c = \frac{\int_{-h/2}^{h/2} P(\bar{z}) \bar{z} d\bar{z}}{\int_{-h/2}^{h/2} P(\bar{z}) d\bar{z}} \quad (3)$$

For homogeneous beams the parameter c will be zero, accordingly, the variation of the material properties in the new coordinate system can be expressed as:

$$P(z) = (P_U - P_L) \left(\frac{z + c}{h} + 0.5 \right)^k + P_L \quad (4)$$

Finally Young's modulus and thermal expansion coefficient can be presented by:

$$E(z) = (E_U - P_L) \left(\frac{z+c}{h} + 0.5 \right)^k + E_L \quad (5)$$

$$\alpha(z) = (\alpha_U - \alpha_L) \left(\frac{z+c}{h} + 0.5 \right)^k + \alpha_L \quad (6)$$

2.2 Nonlocal Strain Gradient Theory (NSGT)

On the basis of nonlocal strain gradient proposed by Lim et al. (2015), the total stress tensor accounts for not only nonlocal stress tensor but also strain gradient stress tensor:

$$t_{xx} = \sigma_{xx} - \nabla \sigma_{xx}^{(1)} \quad (7)$$

Where $\nabla = \partial/\partial x$ is differential operator, t_{xx} , σ_{xx} , $\sigma_{xx}^{(1)}$ are the total stress, the classical stress tensor and the higher-order stress tensor, respectively. The more general nonlocal strain gradient constitutive relation for a one-dimensional structure can be given as:

$$[1 - (e_1 a)^2 \nabla^2][1 - (e_0 a)^2 \nabla^2] t_{xx} = E[1 - (e_1 a)^2 \nabla^2] \varepsilon_{xx} - E l^2 [1 - (e_0 a)^2 \nabla^2] \nabla^2 \varepsilon_{xx} \quad (8)$$

Here $\nabla^2 = \partial^2/\partial x^2$ is the Laplacian operator, $e_0 a$ and $e_1 a$ are the influences of nonlocal stress field, and l refers to the material length scale parameter capturing the effects of higher-order strain gradient stress field. Supposing $e = e_0 = e_1$, the general equation can be simplified as:

$$[1 - (ea)^2 \nabla^2] t_{xx} = E[1 - l^2 \nabla^2] \varepsilon_{xx} \quad (9)$$

The constitutive Eq. (9) can be developed to capture the effect of thermal loading as below:

$$[1 - (ea)^2 \nabla^2] t_{xx} = E[1 - l^2 \nabla^2] \varepsilon_{xx} - \alpha \theta \quad (10)$$

In which α is thermal expansion coefficient and θ is temperature variation. The nonlocal strain gradient governing equation given in Eq. (10) states that the stress accounts for both nonlocal stress field (Eringen, 1983), and the higher-order pure strain gradient stress field (Aifantis, 1992). The nonlocal strain gradient model has two independent small length-scale parameters (i.e., the nonlocal parameter and the material length scale parameter). The nonlocal and material length scale parameter parameters are responsible for capturing the effect of nonlocal elastic stress field and strain gradient stress fields, respectively.

2.3 Equation derivation

The non-zero component of the geometrically nonlinear strain tensor for an Euler–Bernoulli beam can be formulated as:

$$\varepsilon_{xx} = \frac{\partial u(x)}{\partial x} + \frac{1}{2} \left(\frac{\partial w(x)}{\partial x} \right)^2 - z \frac{\partial^2 w(x)}{\partial x^2} \quad (11)$$

where $u(x)$ and $w(x)$ denote the axial and transverse displacements at the mid plane, respectively. The virtual strain energy on the basis of nonlocal strain gradient theory can be written as:

$$\delta U = \int_V \sigma_{xx} \delta \varepsilon_{xx} + \sigma_{xx}^{(1)} \nabla \delta \varepsilon_{xx} dV = \int_V t_{xx} \delta \varepsilon_{xx} dV + \left[\int_V \sigma_{xx}^{(1)} \delta \varepsilon_{xx} dA \right]_0^L \quad (12)$$

where A is the area of the cross-section. Substituting Eq. (11) in Eq. (12) yields:

$$\delta U = \int_0^L \left[N_c \left(\frac{\partial}{\partial x} \delta u + \frac{\partial w}{\partial x} \frac{\partial}{\partial x} \delta w \right) - M_c \left(\frac{\partial^2}{\partial x^2} \delta w \right) \right] dx + \left[N_{nc} \left(\frac{\partial}{\partial x} \delta u + \frac{\partial w}{\partial x} \frac{\partial}{\partial x} \delta w \right) - M_{nc} \left(\frac{\partial^2}{\partial x^2} \delta w \right) \right]_0^L \quad (13)$$

N and M refer to normal force and moment and indexes c and nc are the abbreviations of classic and non-classic, respectively.

$$N_c = \int_A t_{xx} dA, M_c = \int_A z t_{xx} dA, N_{nc} = \int_A \sigma_{xx}^{(1)} dA, M_{nc} = \int_A z \sigma_{xx}^{(1)} dA \quad (14)$$

The variation of the work done by the external force $Q(x)$ is expressed as:

$$\delta W = \int_0^L Q(x) \delta w dx = 0 \quad (15)$$

In order to derive the governing equations, minimum total potential energy principle is utilized:

$$\delta U - \delta W = 0 \quad (16)$$

By employing Eqs. (13) and (15) into Eq. (16), setting the coefficients of δu and δw equal to zero, the Euler–Lagrange equations in $0 < x < L$ based on the Euler–Bernoulli beam theory in the framework of nonlocal strain gradient theory can be obtained as:

$$\delta u : \frac{\partial}{\partial x} N_c = 0 \quad , \quad \delta w : \frac{\partial^2 M_c}{\partial x^2} + \frac{\partial}{\partial x} \left(N_c \frac{\partial w}{\partial x} \right) + Q = 0 \quad (17)$$

In order to obtain deflection equation of FG nano-beam in terms of displacement, first two sides of the Eq. (10) is integrated with respect to the cross-section area:

$$\begin{aligned} N_c - (ea)^2 \frac{\partial^2 N_c}{\partial x^2} &= A_0 \left[\frac{\partial u}{\partial x} + \frac{1}{2} \left(\frac{\partial w}{\partial x} \right)^2 \right] - B_0 \frac{\partial^2 w}{\partial x^2} - A_0 l^2 \left[\frac{\partial^3 u}{\partial x^3} + \frac{\partial w}{\partial x} \frac{\partial^3 w}{\partial x^3} + \left(\frac{\partial^2 w}{\partial x^2} \right)^2 \right] \\ &+ B_0 l^2 \frac{\partial^4 w}{\partial x^4} - \int_A E(z) \alpha(z) \theta dA \end{aligned} \quad (18)$$

Second, both sides of Eq. (10) is multiplied to z then integrated over the cross-section area:

$$\begin{aligned} M_c - (ea)^2 \frac{\partial^2 M_c}{\partial x^2} &= B_0 \left[\frac{\partial u}{\partial x} + \frac{1}{2} \left(\frac{\partial w}{\partial x} \right)^2 \right] - B_0 l^2 \left[\frac{\partial^3 u}{\partial x^3} + \frac{\partial w}{\partial x} \frac{\partial^3 w}{\partial x^3} + \left(\frac{\partial^2 w}{\partial x^2} \right)^2 \right] \\ &- C_0 \frac{\partial^2 w}{\partial x^2} + C_0 l^2 \frac{\partial^4 w}{\partial x^4} - \int_A E(z) \alpha(z) \theta dA \end{aligned} \quad (19)$$

where the cross-sectional rigidities are calculated as follows:

$$A_0, B_0, C_0 = \int_A E(z) \, 1, z, z^2 \, dA \quad (20)$$

Note that according to the origin of the z axis, B_0 is equal to zero. Moreover, Thermal force and thermal moment are introduced as:

$$N_T, M_T = \int_A E(z)\alpha(z)\theta_{1,z} dA \quad (21)$$

Inserting Eq. (18) into Eq. (17) gives:

$$\frac{\partial u}{\partial x} + \frac{1}{2} \left(\frac{\partial w}{\partial x} \right)^2 - l^2 \left[\frac{\partial^3 u}{\partial x^3} + \frac{\partial w}{\partial x} \frac{\partial^3 w}{\partial x^3} + \left(\frac{\partial^2 w}{\partial x^2} \right)^2 \right] - \frac{1}{A_0} N_T = \frac{C}{A_0} \quad (22)$$

where C is the integration constant to be determined by the boundary conditions. The nano-beam with immovable ends has the following boundary conditions related to the axial motion:

$$u(0) = u(L) = \frac{\partial^2 u(0)}{\partial x^2} = \frac{\partial^2 u(L)}{\partial x^2} = 0 \quad (23)$$

Applying the boundary condition the axial normal force can be found as:

$$N_c = \frac{A_0}{2L} \int_0^L \left(\frac{\partial w}{\partial x} \right)^2 dx - \frac{A_0}{L} l^2 \int_0^L \left[\frac{\partial w}{\partial x} \frac{\partial^3 w}{\partial x^3} + \left(\frac{\partial^2 w}{\partial x^2} \right)^2 \right] dx - \frac{1}{L} \int_0^L N_T dx \quad (24)$$

Substituting N_c into Eq. (18) and using Eq. (19), the static deflection of FG nano-beam is obtained:

$$\begin{aligned} & C_0 l^2 \frac{\partial^6 w}{\partial x^6} - C_0 \frac{\partial^4 w}{\partial x^4} \\ & + \left\{ \frac{A_0}{2L} \int_0^L \left(\frac{\partial w}{\partial x} \right)^2 dx - \frac{A_0}{L} l^2 \int_0^L \left[\frac{\partial w}{\partial x} \frac{\partial^3 w}{\partial x^3} + \left(\frac{\partial^2 w}{\partial x^2} \right)^2 \right] dx - \frac{1}{L} \int_0^L N_T dx \right\} \left(1 - (ea)^2 \frac{\partial^2}{\partial x^2} \right) \frac{\partial^2 w}{\partial x^2} \\ & = \left(1 - (ea)^2 \frac{\partial^2}{\partial x^2} \right) Q \end{aligned} \quad (25)$$

When the actuating voltage is applied between the nano-beam and substrate, the electrostatic force per unit length are computed using a standard capacitance model and expressed by Q_{elct} . For the small/large separation regime, the dispersion force per unit length of the beam is defined considering the VdW/Casimir force (Jafarsadeghi et al. 2014). Consequently, Q is determined as the summation of the electrostatic and intermolecular forces:

$$\begin{aligned} Q &= Q_{elct} + Q_s \\ Q_{elct} &= \frac{\varepsilon_0 b V^2}{2 (g_0 - w)^2}, Q_s = \frac{\Lambda_s}{2 (g_0 - w)^s}, s = 3, 4, \Lambda_3 = \frac{\tilde{A} b}{6\pi}, \Lambda_4 = \frac{\pi^2 \hbar c b}{240} \end{aligned} \quad (26)$$

Where ε_0 , b , g_0 and V is air permittivity, width of the FG nano-beam, the initial gap between the nano-beam and the ground electrode and the applied DC voltage, respectively. Besides, $\tilde{A} = (0.4 - 4) \times 10^{(-19)} J$ is Hamaker's constant, $\hbar = 1.055 \times 10^{34} Js$ is Planck's constant and c is the speed of light. Note that Q_3 denotes Van der Waals force and Q_4 stands for Casimir force per unit length between nano-beam and substrate. Finally, the nonlinear governing static deflection of nonlocal strain gradient FG Euler–Bernoulli nano-beam can be updated as:

$$C_0 l^2 \frac{\partial^6 w}{\partial x^6} - C_0 \frac{\partial^4 w}{\partial x^4} \quad (27)$$

$$\begin{aligned}
& + \left[\frac{A_0}{2L} \int_0^L \left(\frac{\partial w}{\partial x} \right)^2 dx - \frac{A_0}{L} l^2 \int_0^L \left[\frac{\partial w}{\partial x} \frac{\partial^3 w}{\partial x^3} + \left(\frac{\partial^2 w}{\partial x^2} \right)^2 \right] dx - N_T \left[\left(1 - (ea)^2 \frac{\partial^2}{\partial x^2} \right) \frac{\partial^2 w}{\partial x^2} \right] \right. \\
& = (ea)^2 \left[\left(\frac{3\varepsilon_0 b V^2}{(g_0 - w)^4} + \frac{s(s+1)\Lambda_s}{(g_0 - w)^{s+2}} \right) \left(\frac{\partial w}{\partial x} \right)^2 + \left(\frac{\varepsilon_0 b V^2}{(g_0 - w)^3} + \frac{s\Lambda_s}{(g_0 - w)^{s+1}} \right) \frac{\partial^2 w}{\partial x^2} \right] \\
& \quad - \frac{\varepsilon_0 b V^2}{2(g_0 - w)^2} + \frac{\Lambda_s}{(g_0 - w)^s}
\end{aligned}$$

To rearrange the equations into a non-dimensional form Following dimensionless quantities are presented:

$$\hat{x} = \frac{x}{L}, \hat{w} = \frac{w}{g_0}, \hat{z} = \frac{z}{h}, \eta = \frac{ea}{L}, \beta = \frac{l}{L} \quad (28)$$

Therefore, the non-dimensional static deflection equation is rewritten as follow:

$$\begin{aligned}
& \beta^2 \frac{\partial^6 \hat{w}}{\partial \hat{x}^6} - \frac{\partial^4 \hat{w}}{\partial \hat{x}^4} + A_1 [N_I - \beta^2 N_{II} + N_{III}] - \hat{N}_T \left(1 - \eta^2 \frac{\partial^2}{\partial \hat{x}^2} \right) \frac{\partial^2 \hat{w}}{\partial \hat{x}^2} \\
& = \eta^2 \left[\left(\frac{3A_2 V^2}{(1 - \hat{w})^4} + \frac{s(s+1)A_3}{(1 - \hat{w})^{s+2}} \right) \left(\frac{\partial \hat{w}}{\partial \hat{x}} \right)^2 + \left(\frac{A_2 V^2}{(1 - \hat{w})^3} + \frac{sA_3}{(1 - \hat{w})^{s+1}} \right) \frac{\partial^2 \hat{w}}{\partial \hat{x}^2} \right] - \frac{A_2 V^2}{2(1 - \hat{w})^2} + \frac{A_3}{(1 - \hat{w})^s}
\end{aligned} \quad (29)$$

In which:

$$\begin{aligned}
N_I &= \frac{1}{2} \int_0^1 \left(\frac{\partial \hat{w}}{\partial \hat{x}} \right)^2 d\hat{x}, N_{II} = \frac{1}{2} \int_0^1 \frac{\partial \hat{w}}{\partial \hat{x}} \frac{\partial^3 \hat{w}}{\partial \hat{x}^3} d\hat{x}, N_{III} = \frac{1}{2} \int_0^1 \left(\frac{\partial^2 \hat{w}}{\partial \hat{x}^2} \right)^2 d\hat{x} \\
A_1 &= \frac{A_0 g_0^2}{C_0}, A_2 = \frac{\varepsilon_0 b L^4}{C_0 g_0^3}, A_3 = \frac{L^4 \Lambda_s}{C_0 g_0^{s+1}}, \hat{N}_T = \frac{N_T}{C_0 / L}
\end{aligned} \quad (30)$$

3 Solution methodology

The considered method to solve the equation of the static deflection includes two steps. Because of the existence of non-linear terms in Eq. (29), the analytical methods cannot be used to solve the governing equation, therefore, first a step-by-step linearization method (SSLM) is adopted, subsequently, Galerkin weighted residual method is implemented to solve the governing equations of the static deflection. Using this method results in the smooth and continuous behavior of the beam can be approximated in each step and the amount of nonlinear forces in each step will be obtained from former iterations (Rezazadeh 2011). By considering \hat{w}^i as the displacement of the beam due to the applied voltage due to V_i and λ_i (virtual force variable) it can be concluded that the deflection of \hat{w}^{i+1} is:

$$\begin{cases} V_{i+1} = V_i + \delta V \\ \lambda_{i+1} = \lambda_i + \delta \lambda \end{cases} \Rightarrow \hat{w}^{i+1} = \hat{w}^i + \delta w = \hat{w}^i + \Psi(\hat{x}) \quad (31)$$

$$\beta^2 \frac{\partial^6 \hat{w}^{i+1}}{\partial \hat{x}^6} - \frac{\partial^4 \hat{w}^{i+1}}{\partial \hat{x}^4} + A_1 [N_I^{i+1} - \beta^2 N_{II}^{i+1} + N_{III}^{i+1}] - \hat{N}_T \left(1 - \eta^2 \frac{\partial^2}{\partial \hat{x}^2} \right) \frac{\partial^2 \hat{w}^{i+1}}{\partial \hat{x}^2} \quad (32)$$

$$\begin{aligned}
&= \eta^2 \left[\left(\frac{3A_2 V_{i+1}^2}{(1-\hat{w}^{i+1})^4} + \frac{s(s+1)A_3 \lambda_{i+1}}{(1-\hat{w}^{i+1})^{s+2}} \right) \left(\frac{\partial \hat{w}^{i+1}}{\partial \hat{x}} \right)^2 + \left(\frac{A_2 V_{i+1}^2}{(1-\hat{w}^{i+1})^3} + \frac{sA_3 \lambda_{i+1}}{(1-\hat{w}^{i+1})^{s+1}} \right) \frac{\partial^2 \hat{w}^{i+1}}{\partial \hat{x}^2} \right] \\
&\quad - \frac{A_2 V_{i+1}^2}{2(1-\hat{w}^{i+1})^2} + \frac{A_3 \lambda_{i+1}}{(1-\hat{w}^{i+1})^s}
\end{aligned}$$

By considering a small values for δV and $\delta \lambda$, $\delta \hat{w}$ will be small enough to use Calculus of Variation theory and Taylor's series expansion around \hat{w}^i . Hence, applying the truncation to first order for suitable values of δV and $\delta \lambda$, it is possible to obtain the desired accuracy.

$$\begin{aligned}
&\beta^2 \frac{\partial^6 \Psi}{\partial \hat{x}^6} - \frac{\partial^4 \Psi}{\partial \hat{x}^4} + A_1 \left[N_I^i - \beta^2 N_{II}^i + N_{III}^i \right] \left(1 - \eta^2 \frac{\partial^2}{\partial \hat{x}^2} \right) \frac{\partial^2 \Psi}{\partial \hat{x}^2} + \delta N_I \left(1 - \eta^2 \frac{\partial^2}{\partial \hat{x}^2} \right) \left(\frac{\partial^2 \hat{w}^i}{\partial \hat{x}^2} + \frac{\partial^2 \Psi}{\partial \hat{x}^2} \right) \\
&- \hat{N}_T \left(1 - \eta^2 \frac{\partial^2}{\partial \hat{x}^2} \right) \frac{\partial^2 \Psi}{\partial \hat{x}^2} = \eta^2 3A_2 \left[\frac{V_i^2}{(1-\hat{w}^i)^4} 2 \left(\frac{\partial \hat{w}^i}{\partial \hat{x}} \right) \left(\frac{\partial \Psi}{\partial \hat{x}} \right) + \frac{4V_i^2}{(1-\hat{w}^i)^5} \Psi \left(\frac{\partial \hat{w}^i}{\partial \hat{x}} \right)^2 + \frac{2V_i \delta V}{(1-\hat{w}^i)^4} \left(\frac{\partial \hat{w}^i}{\partial \hat{x}} \right)^2 \right] \\
&\quad \eta^2 3A_2 \left[\frac{V_i^2}{(1-\hat{w}^i)^4} 2 \left(\frac{\partial \hat{w}^i}{\partial \hat{x}} \right) \left(\frac{\partial \Psi}{\partial \hat{x}} \right) + \frac{4V_i^2}{(1-\hat{w}^i)^5} \Psi \left(\frac{\partial \hat{w}^i}{\partial \hat{x}} \right)^2 + \frac{2V_i \delta V}{(1-\hat{w}^i)^4} \left(\frac{\partial \hat{w}^i}{\partial \hat{x}} \right)^2 \right] \\
&+ \eta^2 s(s+1)A_3 \left[\frac{\lambda_i}{(1-\hat{w}^i)^{s+2}} 2 \left(\frac{\partial \hat{w}^i}{\partial \hat{x}} \right) \left(\frac{\partial \Psi}{\partial \hat{x}} \right) + \frac{(s+2)\lambda_i}{(1-\hat{w}^i)^{s+3}} \Psi \left(\frac{\partial \hat{w}^i}{\partial \hat{x}} \right)^2 + \frac{\delta \lambda}{(1-\hat{w}^i)^{s+2}} \left(\frac{\partial \hat{w}^i}{\partial \hat{x}} \right)^2 \right] \quad (33) \\
&\quad + \eta^2 A_2 \left[\frac{V_i^2}{(1-\hat{w}^i)^3} \left(\frac{\partial^2 \Psi}{\partial \hat{x}^2} \right) + \frac{3V_i^2}{(1-\hat{w}^i)^4} \Psi \left(\frac{\partial^2 \hat{w}^i}{\partial \hat{x}^2} \right) + \frac{2V_i \delta V}{(1-\hat{w}^i)^3} \left(\frac{\partial^2 \hat{w}^i}{\partial \hat{x}^2} \right) \right] \\
&\quad + \eta^2 sA_3 \left[\frac{\lambda_i}{(1-\hat{w}^i)^{s+1}} \left(\frac{\partial^2 \Psi}{\partial \hat{x}^2} \right) + \frac{(s+1)\lambda_i}{(1-\hat{w}^i)^{s+2}} \Psi \left(\frac{\partial^2 \hat{w}^i}{\partial \hat{x}^2} \right) + \frac{\delta \lambda}{(1-\hat{w}^i)^{s+1}} \left(\frac{\partial^2 \hat{w}^i}{\partial \hat{x}^2} \right) \right] \\
&\quad - \frac{A_2}{2} \left[\frac{2V_i^2}{(1-\hat{w}^i)^3} \Psi + \frac{2V_i \delta V}{(1-\hat{w}^i)^2} \right] - A_3 \left[\frac{s\lambda_i}{(1-\hat{w}^i)^{s+1}} \Psi + \frac{\delta \lambda}{(1-\hat{w}^i)^s} \right]
\end{aligned}$$

To calculate the variation of hardening terms following equations should be consider here:

$$\begin{aligned}
I &= \int F \left(w, \frac{\partial w}{\partial x}, \frac{\partial^2 w}{\partial x^2}, \frac{\partial^3 w}{\partial x^3}, x \right) dx \\
\delta I &= \int \left[\frac{\partial F}{\partial w} - \frac{d}{dx} \left(\frac{\partial F}{\partial w'} \right) + \frac{d^2}{dx^2} \left(\frac{\partial F}{\partial w''} \right) - \frac{d^3}{dx^3} \left(\frac{\partial F}{\partial w'''} \right) \right] \delta w dx \quad (34)
\end{aligned}$$

Utilizing the Eq. variation of the hardening term based on Calculus of Variations Theory can be expressed as:

$$\delta N_I = - \int_0^1 \frac{d^2 \hat{w}}{d\hat{x}^2} \Psi d\hat{x}, \quad \delta N_{II} = - \int_0^1 2 \frac{d^4 \hat{w}}{d\hat{x}^4} \Psi d\hat{x}, \quad \delta N_{III} = - \int_0^1 2 \frac{d^4 \hat{w}}{d\hat{x}^4} \Psi d\hat{x} \quad (35)$$

Classification based on the order of terms rearrange Eq. (33) to:

$$\begin{aligned}
&\beta^2 \frac{\partial^6 \Psi}{\partial \hat{x}^6} - \frac{\partial^4 \Psi}{\partial \hat{x}^4} + A_1 \left[N_I^i - \beta^2 N_{II}^i + N_{III}^i \right] - \hat{N}_T \left(1 - \eta^2 \frac{\partial^2}{\partial \hat{x}^2} \right) \frac{\partial^2 \Psi}{\partial \hat{x}^2} + A_1 \delta N_I \left(1 - \eta^2 \frac{\partial^2}{\partial \hat{x}^2} \right) \left(\frac{\partial^2 \hat{w}^i}{\partial \hat{x}^2} \right) \\
&= 2\eta^2 \left[\frac{3A_2 V_i^2}{(1-\hat{w}^i)^4} + \frac{s(s+1)A_3 \lambda_i}{(1-\hat{w}^i)^{s+2}} \right] \left(\frac{\partial \hat{w}^i}{\partial \hat{x}} \right) \left(\frac{\partial \Psi}{\partial \hat{x}} \right) + \eta^2 \left[\frac{12A_2 V_i^2}{(1-\hat{w}^i)^5} + \frac{s(s+1)(s+2)A_3 \lambda_i}{(1-\hat{w}^i)^{s+3}} \right] \Psi \left(\frac{\partial \hat{w}^i}{\partial \hat{x}} \right)^2 \quad (36)
\end{aligned}$$

$$\begin{aligned}
& +\eta^2 \left[\frac{6A_2V_i\delta V}{(1-\hat{w}^i)^4} + \frac{s(s+1)A_3\delta\lambda_i}{(1-\hat{w}^i)^{s+2}} \right] \left(\frac{\partial\hat{w}^i}{\partial\hat{x}} \right)^2 + \eta^2 \left[\frac{A_2V_i^2}{(1-\hat{w}^i)^3} + \frac{sA_3\lambda_i}{(1-\hat{w}^i)^{s+1}} \right] \left(\frac{\partial^2\Psi}{\partial\hat{x}^2} \right) \\
& +\eta^2 \left[\frac{3A_2V_i^2}{(1-\hat{w}^i)^4} + \frac{s(s+1)A_3\lambda_i}{(1-\hat{w}^i)^{s+2}} \right] \Psi \left(\frac{\partial^2\hat{w}^i}{\partial\hat{x}^2} \right) + \eta^2 \left[\frac{A_22V_i\delta V}{(1-\hat{w}^i)^3} + \frac{sA_3\delta\lambda_i}{(1-\hat{w}^i)^{s+1}} \right] \left(\frac{\partial^2\hat{w}^i}{\partial\hat{x}^2} \right) \\
& -\eta^2 \left[\frac{A_2V_i^2}{(1-\hat{w}^i)^3} + \frac{sA_3\lambda_i}{(1-\hat{w}^i)^{s+1}} \right] \Psi - \left[\frac{A_2V_i\delta V}{(1-\hat{w}^i)^2} + \frac{A_3\delta\lambda_i}{(1-\hat{w}^i)^s} \right]
\end{aligned}$$

As discussed earlier, considering a small value of δV , causes $\Psi(\hat{x})$ have a small value, Therefore, multiplying δN_I to $\partial^2\Psi / \partial\hat{x}^2$ will be small enough to neglect (Rezazadeh 2011). Eq. (36) is a linear differential equation and can be solved using a Galerkin based weighted residual method. By choosing suitable shape functions satisfying the geometrical boundary conditions of the nano-beam $\Psi(\hat{x})$ may be approximated by the following series where a_j are constant coefficients will be calculated at each step,

$$\Psi(\hat{x}) = \sum_{j=1}^n a_j \Phi_j(\hat{x}) \quad (37)$$

4 Static response analysis

In order to analyze the system behavior, the beam parameters in this study are set similar to a typical system widely used in Osterberg and Senturia (1997). Herein the beam's geometric and material properties are given as follows: Young's modulus is 169 GPa, width of the beam is 50 μm , thickness of the beam is 3 μm , initial gap is 1 μm . Considering the data of Tab.1, the validity of present mathematical modeling can be established. Table 2 presents the geometric, material and air properties of FG capacitive nano-beam.

Table 1 Comparison of static pull-in voltage [V] for clamped-clamped micro-beams with experimental and numerical data presented in the literatures

References	Beam length (μm)		
	250	350	
Osterberg and Senturia (1997)	(Energy model)	39.5	20.2
	(MEMCAD)	40.1	20.3
Sadeghian et al. (2007)		39.13	20.36
Rezazadeh et al. (2011)		39.5	20.1
Rokni and Lu (2013)		39.40	20.1
Tavakolian et al. (2017)		39.34	20.1
Present study	(without stretching)	39.26	20.07
	(considering stretching)	39.42	20.14

Table 2 Geometrical, material and air properties of micro-beam

Symbols	Parameters	Value/unit	
L	Length	50 [nm]	
b	Width	10 [nm]	
h	Thickness	5 [nm]	
g_0	Initial gap	5 [nm]	
E	Young's modulus	Metal (steel)	210 [Gpa]
		Ceramic (Al_2O_3)	390 [Gpa]
α	Thermal expansion	Metal (steel)	12.5×10^{-6} [K^{-1}]
		Ceramic (Al_2O_3)	8.5×10^{-6} [K^{-1}]
ϵ_0	Permittivity of air	8.85×10^{-12} [$C^2N^{-1}m^{-2}$]	

In accordance with the power-law distribution of a material's property given by Eqs. (5) and (6), variation of the Young's modulus and thermal expansion coefficient through the beam thickness with different material-variation profile parameter k is presented in Fig. 2. It is obvious that, as the material gradient index changes from 0.2 to 5, the material graduation is changed from pure isotropic alumina (Al_2O_3) to approximately pure steel.

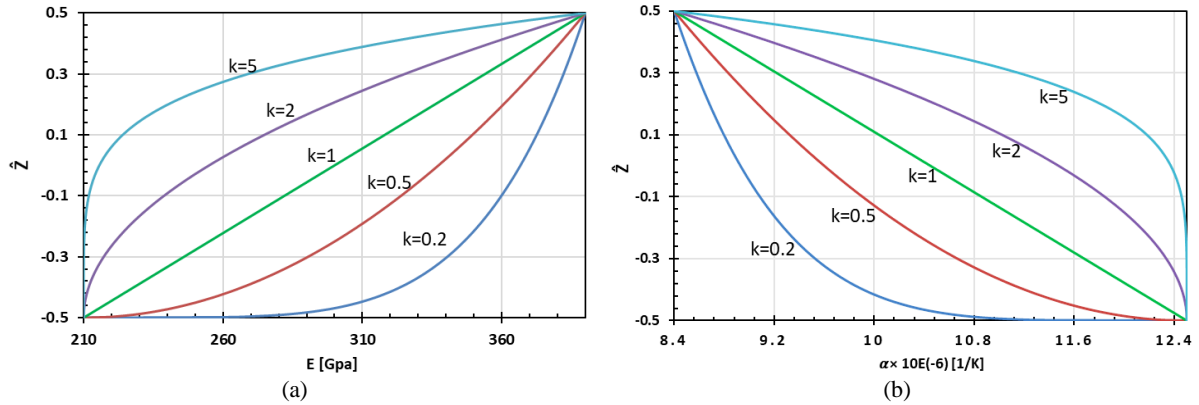


Fig. 2 The variation of Young's modulus (a) and thermal expansion coefficient (b) through the nano-beam thickness for different values of k .

When the gap between stationary electrode and movable FG nano-beam is small enough, the movable beam might collapse onto the stationary electrode without applying voltage due to the Casimir or VdW force having $k = 1$. Figures 3 shows the effect of Casimir and VdW forces on the bending of FG nano-beam, for different gaps when there is no electrostatic pressure and the beam is deflected only by applying the intermolecular forces. The figure reveals that, firstly, for the gaps considered here, when the beam is exposed to Casimir dispersion force, the deflection of mid-point is larger than applying VdW dispersion one. Furthermore, according to the Ramezni et al. (2008) and Koochi et al. (2010), the detachment gap (the minimum gap in which the deformable beam does not jump and stick to the stationary electrode before applying of bias voltage) for the fixed length is about 3.5 [nm]. Thirdly, because of the nonlinear nature of these forces, as the gap increases, the non-dimensional deflection decreases. Henceforth, the results are obtained applying Casimir force.

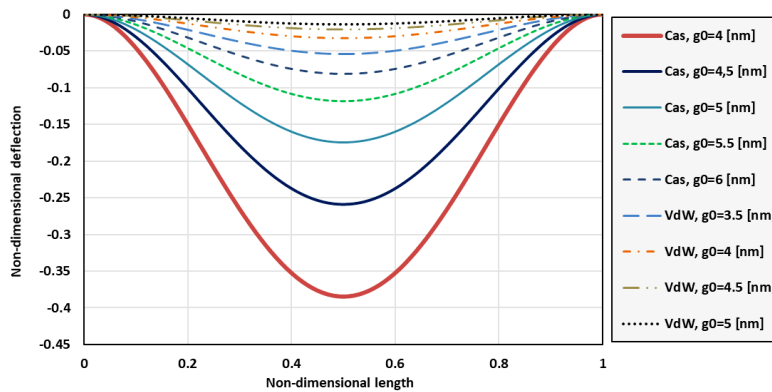


Fig. 3 Non-dimensional deflection of clamped-clamped FG nano-beam for different gaps when $k=1$: effect of intermolecular forces.

In conjunction with Fig.3, the plotted results in Fig. 4 demonstrate the effect of non-dimensional nonlocal parameter and non-dimensional size effect on the static deflection of FG nano-beam. As seen from the figure, considering size effect gives smaller deflection due to increasing in the rigidity of nano-beam. This phenomena indicates that the FG nano-beam exerts a stiffness-hardening effect when the length scale parameter is included in the model. In contrary, increasing nonlocal parameter decreases stiffness of the beams and it causes the rise of bending in the beam. In other words, nonlocality applies a stiffness-softening effect to the beam.

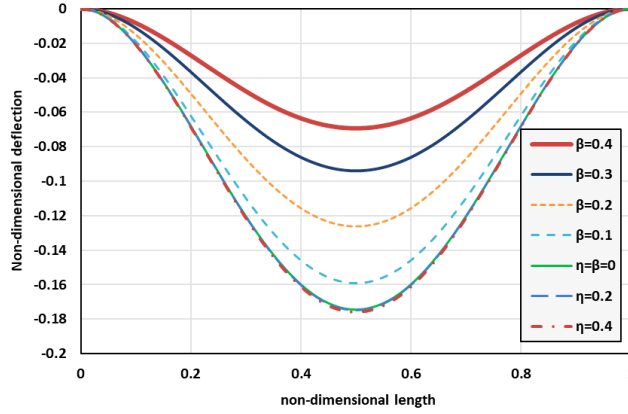


Fig. 4 Non-dimensional deflection of clamped-clamped FG nano-beam for $k = 1$: effect of non-dimensional nonlocal and size effect parameters.

With increasing DC voltage the amplitude of the FG nano-beam mid-point deflection increases until a specific voltage. At this point, a saddle-node bifurcation occurs which leads the system to an unstable position; this phenomenon in NEMS/MEMS resonators is known as the static pull-in instability and the corresponding voltage is known as the static pull-in voltage. Center deflection of the FG nano-beam versus applied voltage is shown in Figs. 3 for different values of material exponent via the classic theory. Comparing the pull-in voltage values presented in these figures, can indicate the effect of geometric nonlinearity. Fig. 3b is plotted when the stretching effect is neglected (i.e. linear analysis). It is explicit that for fixed values of k , the pull-in voltages obtained from the nonlinear analysis are larger than those acquired from the linear analysis which is consistent with the observations reported in (Rezazadeh 2011). It is because of hardening effect thanks to the mid-plane stretching.

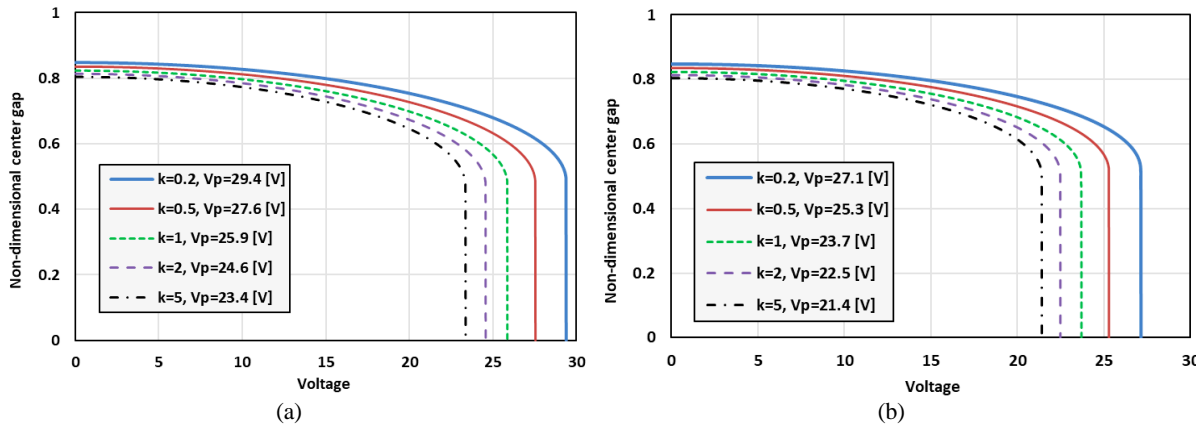


Fig. 5 Non-dimensional center gap of FG nano-beam versus voltage: (a) nonlinear system, (b) linear system.

Figure 6 presents the influence of various initial gaps on the static pull-in voltages for the FG nano-beam having $k = 1$ in the framework of classic theory. As discussed formerly, the beam is primarily deflected due to the Casimir force interacting between two parallel plates. In accordance with the equations of electrostatic and Casimir forces introduced in previous section, increasing the initial gap decreases these forces. The data would seem to suggest that, the less the Casimir force, the less the primal deflection of mid-point, in addition, the less the electrostatic force, the less the deflection of mid-point, and consequently, the more the pull-in voltage value. It should be noticed that electrostatic force reduces the stiffness of the capacitive beam. By taking the electrostatic and Casimir forces into consideration, it is obvious that both of the forces have nonlinear nature regarding to the existence of deflection component into their corresponding equations. These nonlinear natures are responsible for occurring the pull-in phenomenon. Indeed, Casimir force acts both before and after applying bias voltage.

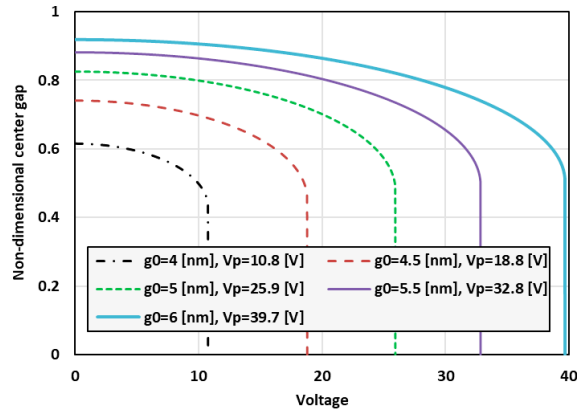


Fig. 6 Non-dimensional center gap of FG nano-beam versus voltage for $k = 1$: effect of different gaps.

Figures below clarify the effect of temperature on static behavior of the system and emphasize the significance of the thermal-induced stresses on the behavior of FG nano resonator. The non-dimensional center gap variation versus increase of the applied voltage for different operating temperatures is presented in Fig. 7, when $k = 1$. Figure 2 shows the pull-in voltage with respect to positive and negative temperature considering different values of power-law exponent. The figures indicate that increasing/reduction of temperature leads to the reduction/increasing of the FG nano-beam pull-in voltage value.

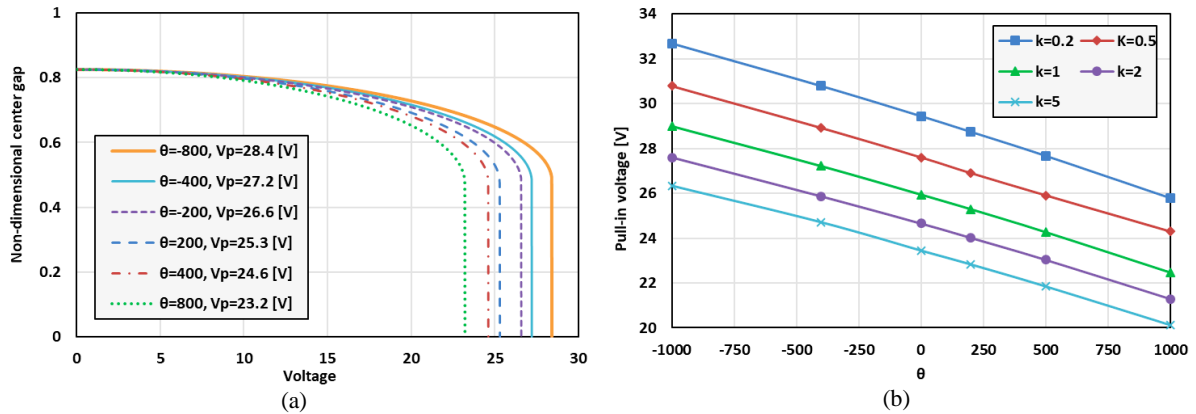


Fig.7 Effect of temperature: (a) Non-dimensional center gap of FG nano-beam versus voltage for $k = 1$, (b) pull-in voltage versus temperature for different material indexes.

Following figures depict the curves of pull-in voltages of FG nano-beam versus non-dimensional nonlocal stress gradient parameter and the non-dimensional strain gradient parameter separately. Thanks to the softening effect observed in the nonlocal elasticity theory, the nonlinear static pull-in voltage reduces with the increase of the nonlocal stress gradient parameter (η). Instead, an increase in the non-dimensional strain gradient parameter (β) leads to enhancement of the pull-in voltage value due to the hardening effect.

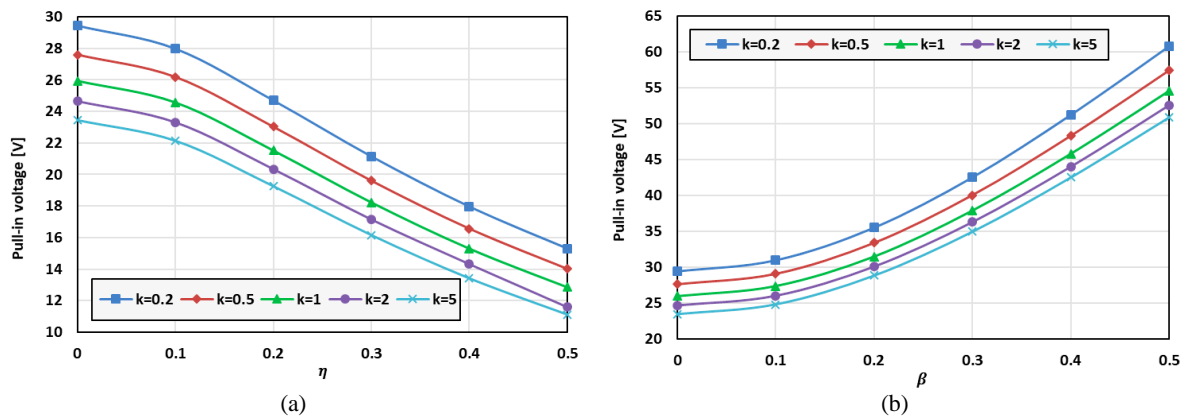


Fig. 8 Pull-in voltage of FG nano-beam: (a) effect of non-dimensional nonlocal parameter, (b) effect of non-dimensional length scale parameter

To obtain a better understanding of FG electrostatic nano-bridge behavior in NSGT, Figs. (9) show the pull-in voltage in respect of length for $k = 1$. In these figures, it is obvious that with increase of the length, static pull-in value decreases for all values of η and β . Fig. (9a) illustrates curves of the pull-in voltage for different values of β and constant value of η considered equal to 0.1, in a similar way, Fig. (9b) depicts curves of pull-in voltage for different values of η and fixed value of β equal to 0.1. Based on explanations rendered previously, as expected, β and η add stiffness and softness to the system, respectively, in which in smaller beam length, the influence of these non-dimensional parameters appears ever more. Note that, associated with the detachment gap expressed before, there is a parameter which is the other basic design parameters in NEMS, called detachment length (the maximum length in which the deformable beam does not jump and stick to the stationary electrode before applying of bias voltage). For the assumed material index and the fixed value of gap (equal to 5 [nm]) in this system, the detachment length when $\eta = \beta = 0$ is almost 80 [nm]. Figures also reveals the convincing effect of small-scale parameters, in the way that, η and β lessen and lift up amount of the detachment length, respectively.

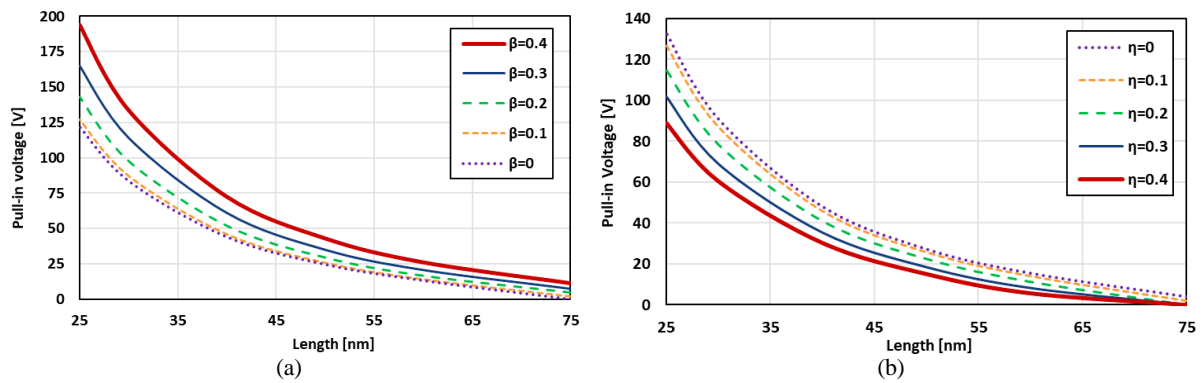


Fig.9 Pull-in voltage of FG nano-beam versus length for $k = 1$: (a) $\eta = 0.1$, (b) $\beta = 0.1$.

Finally Table 3 lists static pull-in voltages for different values of the material gradient exponent, scale parameters and temperature. The data point out that simultaneous applying of these effects cause the static pull-in voltage undergo the wide range of variation. What is interesting in this data is that, in room temperature ($\theta = 0$), when the scale parameters are equal and nonzero ($\beta = \eta \neq 0$), the obtained static pull-in voltages become approximately the same as the results obtained considering the classical theory. The explanation of this consequence is that the softening and hardening effects counteract and cancel each other when both non-dimensional strain and stress gradient parameters are equal to each other. However, for nonzero temperatures this phenomenon cannot be seen. In negative thermal environments, increasing of the scale parameters in the way of $\beta = \eta$, results in the increase in pull-in voltages which means hardening effect of β overcomes softening effect of η . On the contrary, in positive thermal environments, increasing of scale parameters in the way of $\beta = \eta$, causes pull-in voltages to decrease. It means that, in this case softening of η overcomes hardening effect of β .

Table 3 Pull-in voltage values of FG nano-beam for different values of scale parameters in thermal environment

θ	β	$k=0.2$				$k=1$				$k=5$				
		$\eta \Rightarrow$	0.1	0.2	0.3	0.4	0.1	0.2	0.3	0.4	0.1	0.2	0.3	0.4
-500	0.1		31.6	29.4	27.3	25.7	27.9	25.9	24	22.6	25.4	23.5	21.7	20.4
	0.2		35.5	32.4	29.4	27.1	31.6	28.6	25.8	23.7	28.9	26.2	23.6	21.7
	0.3		41.9	37.7	33.5	30.4	37.3	33.4	29.6	26.7	34.5	30.8	27.3	24.5
	0.4		49.9	44.5	39.3	35.2	44.6	39.6	34.9	31.1	41.5	36.8	32.3	28.8
0	0.1		29.4	25.7	21.6	17.9	25.8	22.3	18.5	15.1	23.4	20.1	16.6	13.4
	0.2		33.5	28.8	23.8	19.3	29.5	25.1	20.4	16.2	27	22.9	18.5	14.5
	0.3		40.1	34.4	28.5	23.3	35.5	30.2	24.6	19.7	32.7	27.8	22.5	17.9
	0.4		48.3	41.7	34.9	29.5	42.9	36.8	30.4	25	39.9	34.2	28.2	22.9
500	0.1		27	21.3	13.7	2.85	23.5	18.1	10.8	1.7	21.2	16	9.1	0
	0.2		31.3	24.7	16.6	7.55	27.3	21.1	13.3	4.3	24.9	19	11.6	2.85
	0.3		38.1	30.8	22.3	14.1	33.5	26.6	18.7	10.6	30.8	24.4	16.8	9
	0.4		46.5	38.6	29.8	21.4	41.2	33.8	25.5	17.6	38.2	31.2	23.3	15.8

5 Conclusions

The present work was concerned with developing a numerical model of nano-scaled FG clamped-clamped beam for the static pull-in analysis in combination with the nonlinear geometric effect resulting from mid-plane stretching based on the nonlocal strain gradient theory, in which the stress accounts for not only the nonlocal elastic stress field but also the strain gradients stress field. In the light of the illustrative numerical results, the most important remarks can be summarized as follows:

- The variation of a material property can be enhanced via manipulating the control parameter k .
- Non-dimensional nonlocal parameter/material length scale parameter reduced/increased the static pull-in value as a result of the stiffness-softening/stiffness-hardening effect.
- When the beam was exposed to Casimir force the deflection was larger than that of VdW. Besides, because of the nonlinear nature of these forces, as the gap increased the deflection decreased.
- Decreasing of length leads enhancing of stability, also in smaller beam length, the effect of non-dimensional parameters appears more and more.
- If the length(gap) was more(less) the detachment length(gap), pull-in phenomenon occurred.
- The pull-in voltages obtained by classic and the non-classic theories are the same when both scale parameters are equal to each other.
- In the case of nano-bridge, applying positive/negative temperature variation reduced/enhanced the pull-in voltage. Moreover, in the presence of positive/negative thermal variations, when the scale parameters had the same values, an/a increment/declination in the pull-in voltage values was observed, despite of the zero thermal environment.

References

- Aifantis E C (1992) On the role of gradients in the localization of deformation and fracture. *Int. J. Eng. Sci.* 30:1279–1299
- Ataei H, Tadi Beni Y (2016) Size-dependent pull-in instability of electrically actuated functionally graded nano-beams under intermolecular forces. *Iranian J Sci Technol Trans Mech Eng* 40(4):289–301
- Ebrahimi F, Barati MR (2017) A nonlocal strain gradient refined beam model for buckling analysis of size-dependent shear-deformable curved FG nanobeams. *Compos Struct* 159:174–182
- Ebrahimi F, Dabbagh A (2017) On flexural wave propagation responses of smart FG magneto-electro-elastic nanoplates via nonlocal strain gradient theory. *Compos Struct* 162(15):281–293
- Eringen AC (1983) On differential equations of nonlocal elasticity and solutions of screw dislocation and surface waves. *J Appl Phys* 54(9):4703–4710
- Jafarsadeghi-pournaki I, Rezazadeh G, Zamanzadeh, MR, Shabani R (2014) Thermally induced vibration of an electro-statically deflected functionally graded micro-beam considering thermo-elastic coupling effect, *Scientia Iranica B* 21(3):647–662
- JafarSadeghi-Pournaki I, Zamanzadeh MR, Madinei H, Rezazadeh G (2014) Static pull-in analysis of capacitive FGM nanocantilevers subjected to thermal moment using Eringen's nonlocal elasticity. *IJE trans A* 27(4):633–642
- Karimpour I, Tadi Beni, Y, Koochi, A, AbadyanM (2015) Using couple stress theory for modeling the size-dependent instability of double-sided beam-type nanoactuators in the presence of Casimir force. *J Braz. Soc. Mech. Sci. Eng.* 38(6): 1779–1795.
- Kooch A, Sadat Kazemi A, Tadi Benu Y, Yekrangi A, Abadyan MR (2010) Theoretical study of the effect of Casimir attraction on the pull-in behavior of beam-type NEMS using modified Adomian method. *Phys E* 43:625–632
- Li L, Hu Y (2015) Buckling analysis of size-dependent nonlinear beams based on a nonlocal strain gradient theory. *Int J Eng Sci* 97:84–94
- Li L, Li X, Hu Y (2016) Free vibration analysis of nonlocal strain gradient beams made of functionally graded material, *Int J Eng Sci* 102:77–92
- Lu L, Guo X, Zhao J (2016) Size-dependent vibration analysis of nanobeams based on the nonlocal strain gradient theory. *Int J Eng Sci* 116: 12–24
- Lim CW, Zhang G, Reddy JN (2015) A higher-order nonlocal elasticity and strain gradient theory and its applications in wave propagation. *J Mech Phys Solids* 78:298–313
- Mousavi T, Bornassi S, Haddadpour H, (2012) The effect of small scale on the pull-in instability of nano-switches using DQM. *Int J Solids Struct* 50:1193–1202
- Maani Miandoab E, Yousef Koma, A, Nejat Pishkenari H (2015) Nonlocal and strain gradient based model for electrostatically actuated silicon nano beams. *Microsyst Technol* 21(2):457–464
- Osterberg PM, Senturia SD (1997) M-TEST: a test chip for MEMS material property measurement using electrostatically actuated test structures. *J Microelectromech Syst* 6(2):107–118
- Ramezani A, Alasti A, Akbari j (2008) Analytical investigation and numerical verification of Casimir effect on electrostatic nano-cantilevers. *Microsyst Technol* 14:145–157
- Rezazadeh G, Fathalilou M, Sadeghi M (2011) Pull-in voltage of electrostatically-actuated microbeams in terms of lumped model pull-in voltage using novel design corrective coefficients. *Sens Imaging* 12:117–131
- Rokni H, Lu W (2013) Surface and thermal effects on the pull-in behavior of doubly-clamped graphene nanoribbons under electrostatic and Casimir loads. *J Appl Mech Trans ASME* 80(6):061014–061019

- Sadeghian H, Rezazadeh G, Osterberg PM (2007) Application of the generalized differential quadrature method to the study of pull-in phenomena of MEMS switches. *J Microelectromech Syst* 16(6):1334–1340
- Şimşek M (2016) Nonlinear free vibration of a functionally graded nanobeam using nonlocal strain gradient theory and a novel Hamiltonian approach. *Int J Eng Sci* 105:12–27
- SoltanRezaee M, Afrashi M (2016) Modeling the nonlinear pull-in behavior of tunable nano-switches. *Int J Eng Sci* 109:73-87
- SoltanRezaee M, Farrokhhabadi A, Ghazavi MR (2016) The influence of dispersion forces on the size-dependent pull-in instability of general cantilever nano-beams containing geometrical non-linearity. *Int J Mech Sci* 119:114-124
- Tadi Beni Y, Karimipour, I, Abadyan, M (2015) Modeling the instability of electrostatic nano-bridges and nano-cantilevers using modified strain gradient theory. *Appl Math Modell* 39(9):2633-2648
- Taghavi N, Nahvi, H, (2013) Pull-in instability of cantilever and fixed-fixed nano-switches. *Eur J Mech A Solids* 41:123-133
- Tavakolian F, Farrokhhabadi A, Mirzaei M (2017) Pull-in instability of double clamped micro-beams under dispersion forces in the presence of thermal and residual stress effects using nonlocal elasticity theory. *Microsyst Technol* 23(4):839–848
- Yang WD, Kang WB, Wang X (2017) Scale-dependent pull-in instability of functionally graded carbon nanotubes-reinforced piezoelectric tuning nano-actuator considering finite temperature and conductivity corrections of Casimir force. *Compos Struct* 176(15):460-470
- Yang WD, Yang FP, Wang X (2017) Coupling influences of nonlocal stress and strain gradients on dynamic pull-in of functionally graded nanotubes reinforced nano-actuator with damping effects. *Sens Actuators A Phys* 248(1):10-21
- Zamanzadeh MR, Rezazadeh G, Jafarsadeghi-pournaki I, Shabani R (2013) Static and dynamic stability modeling of a capacitive FGM micro-beam in presence of temperature changes. *Appl Math Modell* 37:6964–6978